Temperature Controlled Perfect Absorber Based on Metal-Superconductor-Metal Square Array

Huang-Ming Lee[1,2] and Jong-Ching Wu[1]

[1]Department of Physics, National Changhua University of Education, Changhua 500, Taiwan
[2]Institute of Physics, National Chiao Tung University, Hsinchu 300, Taiwan

The optical properties of a single-band near-perfect absorber are studied numerically by using a finite element method in conjunction with a two-fluid model. Based on a metal-superconductor-metal (MSM) scheme, the proposed structure comprises a lossless superconducting layer sandwiched by a silver square array and ground silver plane. The simulation results clearly show that near-perfect absorption band can be realized and promptly tuned from green light to red light by the temperature of the system. The designed MSM absorber also presents the characteristics of polarization insensitivity and wide-angle incidence up to 50 degree. This prompt manipulation of the near-perfect absorption band makes this MSM absorber a great potential candidate when designing an in-situ absorption band selector in the visible light wavelength regime.

***Index Terms*—Dipolar resonance, perfect absorber, superconductor.**

I. Introduction

METAMATERIAL absorbers have recently drawn considerable interest due to their near-perfect absorptive efficiency, wide-angle incidence properties, and an almost complete absence of sensitivity to polarization [1]–[6]. These near-perfect absorbers are mostly made from arrays of metal-dielectric-metal (MDM) nanostructures, where the resonant absorption peak wavelength is much greater than the lattice constant of the nanostructures to prevent high order diffraction. MDM absorbers typically consist of three functional layers that comprise a dielectric layer sandwiched between two metal layers. The top layer is mainly a periodically patterned metallic nanostructure that serves as an electric resonator. The bottom layer is mostly a thick metal plane which is employed as an optical mirror that greatly reduces transmittance. The near-perfect absorption bands are attributed to the MDM design that permits the excitation of localized magnetic and electric dipolar resonances. Thus far, the near-perfect MDM absorbers have been investigated from microwave to optical frequencies with single-band [1]–[3], dual-band [4], triple-band [5], and broad-band [6] absorptions, in which the near-perfect absorption bands can be passively tuned only by the geometric dimensions of the MDM nanostructures. To have in-situ manipulation of the absorption band, however, one needs to reconsider new material system with tunable dielectric properties.

In this article, we propose a plasmonic absorber in which the dielectric layer in a conventional MDM structure is replaced by a superconducting layer. The dielectric function of the superconductor [7]–[10] is governed by ambient temperature of the system and frequency of the incident light. By changing system temperature, the metal-superconductor-metal (MSM) absorber exhibits tunable single near-perfect absorption band over the visible light range. Furthermore, the simulation results clearly show that MSM absorber has the properties of polarization insensitivity and wide-angle incidence especially for transverse electric (TE) polarization wave.

Manuscript received March 01, 2012; accepted April 12, 2012. Date of current version October 19, 2012. Corresponding author: J.-C. Wu (e-mail: phjcwu@cc.ncue.edu.tw).

Color versions of one or more of the figures in this paper are available online at http://ieeexplore.ieee.org.

Digital Object Identifier 10.1109/TMAG.2012.2196416

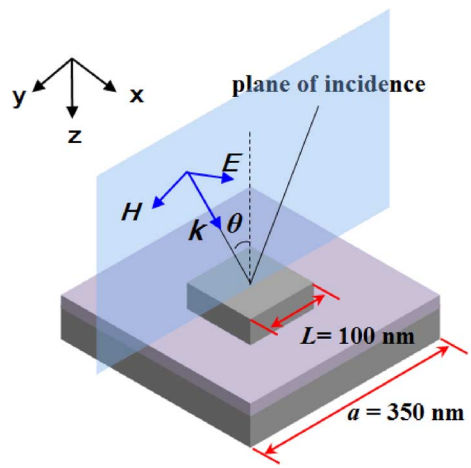

Fig. 1. Schematic drawing of the metal-superconductor-metal absorber structure and the incident TE polarization wave.

II. Numerical Design and Approach

The absorbance properties of the MSM absorber are numerically studied by finite-element method [11]. The MSM structures which are periodically arranged in a square lattice on the x–y plane can be effectively reduced to a simple modeling unit cell with period a as shown in Fig. 1. A 10 nm-thick superconducting layer is sandwiched between two thick sliver metal layers. The top silver layer with a thickness of 40 nm comprising a square with side length denoted as L is responsible for electric dipolar resonance. The bottom silver plane with a thickness of 50 nm exhibits two significant functions. The first function is to serve as an optical mirror with a thickness that is greater than the penetration depth of the incident light in order to zero (zero is a verb, not a adjective) transmittance. The second function is to couple with top silver square to create electric and magnetic

dipolar resonances which dramatically concentrate electromagnetic energy into the MSM nanostructure. L and a are kept constant at 100 and 350 nm, respectively, for all of the following simulations.

Two-fluid model is employed to describe the electromagnetic response of a superconductor with zero magnetic field [12]. The complex conductivity of the superconductor can be expressed as

$$\sigma = \sigma_1 - j\sigma_2 \tag{1}$$

where the real part σ_1 represents the loss and is contributed from the normal electrons, while the imaginary part σ_2 is from the superconducting electrons. The imaginary part is written as the following formula:

$$\sigma_2 = \frac{1}{\omega\mu_0\lambda_p^2} \tag{2}$$

where ω is the angular frequency, μ_0 is permeability in vacuum, and the temperature-dependent penetration depth $\lambda_{\rm p}$ is given by

$$\lambda_p = \frac{\lambda_0}{\sqrt{[1-f(T)]}} \tag{3}$$

where λ_0 is the London penetration depth at temperature $T = 0$ K and the Gorter-Casimir expression $f(T)$ is described by

$$f(T) = \left(\frac{T}{T_c}\right)^p \tag{4}$$

where $T_{\rm c}$ is the superconducting critical temperature and the exponent p depends on the superconducting materials. In this model, the superconductor is Nb ($T_{\rm c} = 9.2$ K, $\lambda_0 = 83.4$ nm) [13], which is classified as low temperature superconducting material with $p = 4$ [14]. For the lossless condition, the real part of the complex conductivity of the superconductor can be ignored, resulting in σ to be expressed as the following formula:

$$\sigma = -j\frac{1}{\omega\mu_0\lambda_p^2}. \tag{5}$$

Deduced by (5), the relative permittivity of the dispersive superconductor can be described by

$$\varepsilon_r = 1 - \frac{1}{\omega^2\mu_0\varepsilon_0\lambda_p^2}. \tag{6}$$

In this simulation, we use Floquet boundary conditions and perfect matched layers to reduce the simulation domain and computation load [15]. The complex dielectric function of silver is interpolated by fitting the data to the curve in Palik's handbook [16]. Two polarized plane waves are used to examine the absorptive properties of the MSM absorber. As shown in Fig. 1, the TE polarized wave with an orientation of electric (E), magnetic (H), and propagation (k) vectors is illuminated on the MSM absorber with an incident angle of θ. Contrary to the TE wave, the H of the transverse magnetic one (TM) is perpendicular to the plane of incidence with E lying on the plane. The near-perfect absorption spectra are then calculated in the visible light wavelength λ ranging from 450 to 750 nm and the incident angle θ ranging up to 50°.

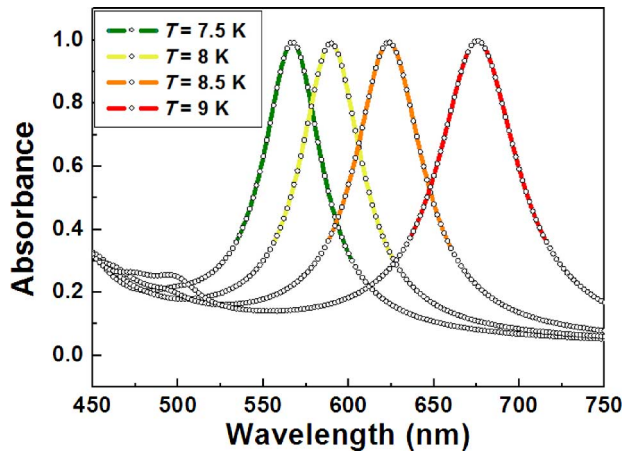

Fig. 2. Absorbance spectra of the MSM absorber taken under normally incident TM (or TE) polarized plane wave. As T increases from 7.5 to 9 K, the absorption peak is shifted from $\lambda = 568$ nm $(A = 99\%)$ to $\lambda = 676$ nm $(A = 99\%)$.

III. Results and Discussion

Fig. 2 shows temperature dependent absorbance spectra of the proposed MSM absorber under normally incident TE (or TM) polarized plane wave. From (6), the electromagnetic response of thin superconducting layer is apparently dependent on ambient temperature of the system and frequency of the incident light. As T increases from 7.5 to 9 K, the near-perfect absorption peak is shifted from $\lambda = 568$ nm $(A = 99\%)$ to $\lambda = 676$ nm $(A = 99\%)$. The corresponding absorption band is promptly tuned from green light to red light without changing the geometry parameters of the MSM although one may also alter the optical properties by different dimensions of the MSM structure [7]–[10]. Note that a redshift behavior of the absorption peak is found and it becomes very sensitive as T is approaching to the vicinity of $T_{\rm c}$ of Nb. This prompt manipulation of the near-perfect absorption band is obviously different from those of the reported works [1]–[6]. This in-situ control makes this MSM absorber more attractive when it comes to design a prompt absorption band selector in the visible light wavelength regime.

Fig. 3 presents the absorbance A as a function of both λ and θ under TE and TM polarized plane waves at $T = 7.5$ K. For TE case as illustrated in Fig. 3(a), the maximum absorption peak at $\lambda = 568$ nm almost remains the same as θ increases up to 50° with A persisting greater than 90%. This superior advantage of wide-angle incidence was also found in the single-band near-perfect MDM absorber in the near-infrared wavelength range [2]. For TM case as shown in Fig. 3(b), however, there exist extra absorption peaks as θ increases greater than 15°. Furthermore, the bandwidth of the TM one becomes narrower as θ increases; absorbance remains 83% as θ increases up to 50°. To sum up, the designed MSM absorber shows the traits of polarization insensitivity and wide-angle incidence when θ is smaller than 50°.

To reveal the physical origin of the near-perfect absorption band in this MSM absorber, the near-field distributions is delineated. Fig. 4 shows near-field profiles in the x–z-plane through the center of the silver square at $\lambda = 568$ nm ($T = 7.5$ K), in which the colormap represents the normalized electric field

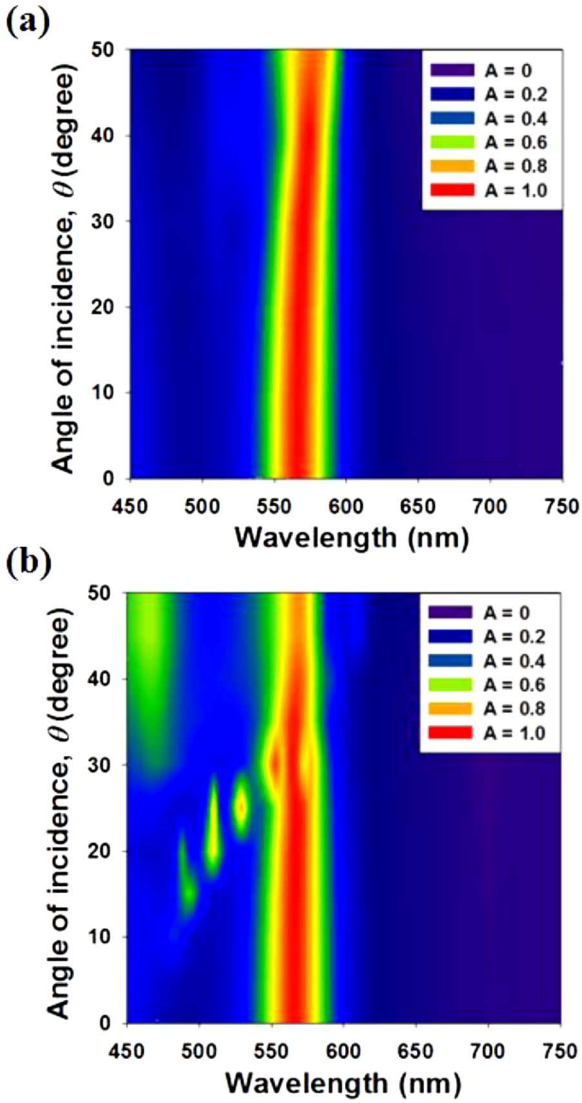

Fig. 3. Contour plots of absorbance (A) as a function of both λ and θ for (a) TE and (b) TM polarized plane waves.

and the white arrows represent the electric displacement vectors. The enhanced electric fields are found to be confined to the space between the silver square and the ground silver plane. The strong confinement of the electric fields is what creates electric dipolar resonance. Moreover, the electric displacement vectors in both the patterned silver layer and the ground silver plane are opposite to each other. The anti-parallel displacement vectors create circulating currents between two metal layers, resulting in artificial magnetic moment that interacts strongly with the magnetic field of the incident light. The strong magnetic dipolar resonances that result from this interaction are then excited between the two metal layers to yield resonant mode. Therefore, the near-perfect absorption band in our single-band absorber is due to the MSM design that permits the excitation of localized magnetic and electric dipolar resonances.

IV. Conclusion

We have numerically delineated the absorption properties of a single-band near-perfect MSM absorber in the visible light

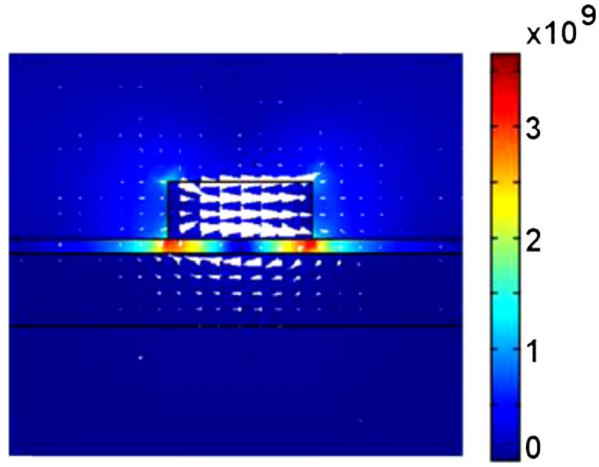

Fig. 4. Near-field profiles in the x–z-plane through the center of the silver square. The colormap represents the normalized electric field and the white arrows represent the electric displacement vectors.

wavelength range. The absorption band under normally incident TE (or TM) polarized plane wave is in-situ tuned from green light ($T = 7.5$ K, $\lambda = 568$ nm, $A = 99\%$) to red light ($T = 9$ K, $\lambda = 676$ nm, $A = 99\%$) without changing the dimensions of the MSM absorber. The designed MSM absorber shows the characteristics of polarization insensitivity and wide-angle incidence when θ is smaller than 50°. The near-perfect absorption band in this absorber is due to the MSM design that permits the excitation of localized magnetic and electric dipolar resonances. This prompt manipulation of the near-perfect absorption band makes this MSM absorber a great potential candidate when it comes to design an absorption band selector in the visible light wavelength regime.

Acknowledgment

This work was supported by the Nation Science Council of the Republic of China (Taiwan) under Grants NSC98-2811-M-018-002, NSC100-2120-M-009-008, and NSC98-2112-M-018-004-MY3.

References

[1] H. Tao, C. M. Bingham, A. C. Strikwerda, D. Pilon, D. Shrekenhamer, N. I. Landy, K. Fan, X. Zhang, W. J. Padilla, and R. D. Averitt, "Highly flexible wide angle of incidence terahertz metamaterial absorber: Design, fabrication, and characterization," *Phys. Rev. B*, vol. 78, p. 241103, Dec. 2008.

[2] J. Hao, J. Wang, X. Liu, W. J. Padilla, L. Zhou, and M. Qiu, "High performance optical absorber based on a plasmonic metamaterial," *Appl. Phys. Lett.*, vol. 96, p. 251104, Jun. 2010.

[3] N. Liu, M. Mesch, T. Weiss, M. Hentschel, and H. Giessen, "Infrared perfect absorber and its application as plasmonic sensor," *Nano Lett.*, vol. 10, pp. 2342–2348, Jun. 2010.

[4] B. Zhang, Y. Zhao, Q. Hao, B. Kiraly, I. C. Khoo, S. Chen, and T. J. Huang, "Polarization-independent dual-band infrared perfect absorber based on a metal-dielectric-metal elliptical nanodisk array," *Opt. Expr.*, vol. 19, pp. 15221–15228, Jul. 2011.

[5] X. Shen, T. J. Cui, J. Zhao, H. F. Ma, W. X. Jiang, and H. Li, "Polarization-independent wide-angle triple-band metamaterial absorber," *Opt. Expr.*, vol. 19, pp. 9401–9407, Apr. 2011.

[6] K. Aydin, V. E. Ferry, R. M. Briggs, and H. A. Atwater, "Broadband polarization-independent resonant light absorption using ultrathin plasmonic super absorbers," *Nat. Commun.*, vol. 2, p. 517, Nov. 2011.

[7] H. M. Lee, C. Y. Lin, L. Horng, and J. C. Wu, "Tunable resonant spectra through nanometer niobium grating on silicon nitride membrane," *J. Appl. Phys.*, vol. 107, p. 09E119, Apr. 2010.
[8] H. M. Lee and J. C. Wu, "Transmittance spectra in one-dimensional superconductor-dielectric photonic crystal," *J. Appl. Phys.*, vol. 107, p. 09E149, May 2010.
[9] H. M. Lee, J. H. Shyu, L. Horng, and J. C. Wu, "Tunable optical properties of a two-dimensional square-lattice superconductor-dielectric Bragg reflector," *Appl. Opt.*, vol. 50, pp. 3860–3864, Jul. 2011.
[10] H. M. Lee, J. H. Shyu, L. Horng, and J. C. Wu, "Surface plasmon polaritons assisted transmission in periodic superconducting grating," *J. Vac. Sci. Technol. B*, vol. 29, p. 04D105, Jun. 2011.
[11] COMSOL RF Module User's Guide [Online]. Available: http://www.comsol.com
[12] M. Tinkham, *Introduction to Superconductivity*, 2nd ed. New York: McGraw-Hill, 1996.
[13] R. L. Kautz, "Picosecond pulses on superconducting striplines," *J. Appl. Phys.*, vol. 49, pp. 308–314, Jan. 1978.
[14] O. G. Vendik, I. B. Vendik, and D. I. Kaparkov, "Emperical model of the microwave properties of high-temperature superconductors," *IEEE Trans. Microw. Theory Tech.*, vol. 46, pp. 469–478, May 1998.
[15] H. M. Lee, L. Horng, and J. C. Wu, "Magnetic-field tunable transmittance in a ferrofluid-filled silicon nitride photonic crystal slab," *J. Phys. D: Appl. Phys.*, vol. 44, p. 064016, Jan. 2011.
[16] E. D. Palik, *Handbook of Optical Constants of Solids*. New York: Academic, 1985.